Observing dust shells of late-type stars with ADONIS

P. Cruzalèbes[1], Y. Rabbia[1], J.D. Monnier[2], and B. Lopez[1]

[1]Observatoire de la Côte d'Azur, Département Fresnel, France
[2]Space Sciences Laboratory, University of California at Berkeley, USA

October 14, 1998

Abstract

We present and discuss late-type star observations we obtained in early Jan.97 with the ADONIS adaptive optic system on the 3.60-m Telescope at ESO-La Silla, Chile. The dust shells surrounding *o* Ceti, VY CMa, V Hya and U Hya have been detected and resolved in J and M with the COMIC camera. We describe their two-dimensional morphology in connection with previous high angular resolution observations and with existing models.

1 Motivation

Our observed late-type stars are evolving along the Asymptotic Giant Branch towards the planetary nebula stage (Fig.1). This evolution is characterized by an ejection of gas and dust. The physical mechanisms which drive the mass loss are still not understood in detail [1]. The morphology of the shell is a good tracer of the history of the mass loss and of the physical mechanisms involved. It has been proved that the mass loss is asymmetric in most cases [2], depending on physico-chemical conditions and on the possible multiplicity of the central star [3]. Adaptive Optics is one of the most relevant tools to undergo this study, mainly because of the angular resolution near the diffraction limit of the telescope.

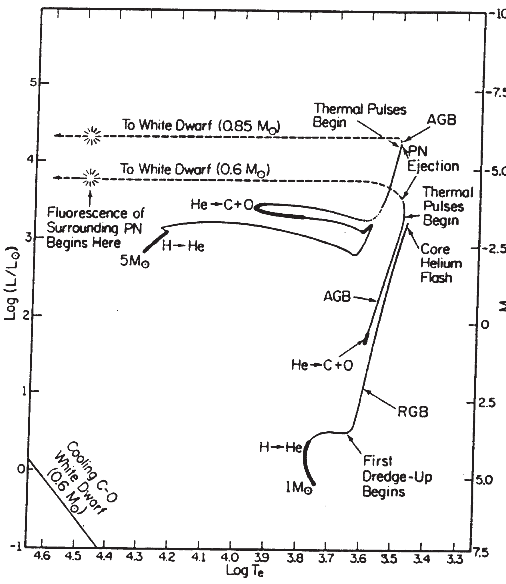

Figure 1: Stellar evolution in the HR diagram of stars with 1 to 9 initial solar masses [4]

2 ADONIS specifications

Adaptive Optic observations allow the detection of faint complex structures in the dust shell, even close to the central star. They provide two-dimensional images necessary to study the morphology of the dust shell. The expected performance of ADONIS is :

- angular resolution close to the diffraction limit of the 3.60-m Telescope
- high dynamic range

3 Observations

Infrared observations of 4 objects and their point-source calibrators have been obtained in Jan.97 using the COMIC camera. The specifications of COMIC are :

- extended spectral sensitivity from 1 to 5 μm
- array format of 128 by 128 pixels
- pixel size allowing a good sampling of the angular resolution

We have alternated observations of the objects and their point-source calibrators in order to calibrate for changing seeing conditions and to eliminate optical residual artefacts by a-posteriori Lucy deconvolution

The observations have been summarized in Tab.1 (end of the paper). Because of the strong brightness of our objects, short-exposure frames had to be stored for each target. Care has been taken to avoid saturation of the COMIC camera and to stay within its linear regim. To reach a good signal to noise ratio in the integrated images, many hundreds to many thousands of frames were collected for each target. Sky cubes were also stored to substract for the background.

4 Results

4.1 δ Ceti

Fig.2 and Fig.3 show the long exposure Shift&Add maps of the point-source calibrator δ Ceti in J, obtained with 2 different adjustments of ADONIS. Fig.2 has been obtained with the current adjustment of ADONIS. Fig.3 has been obtained after we have asked the night assistant for better correcting the residual static "coma" aberration term in the IR way. Lowest contours correspond to 3 times the standard deviation of the noise measured in 10 by 10 pixel boxes situated at the corners of the Shift&Add maps.

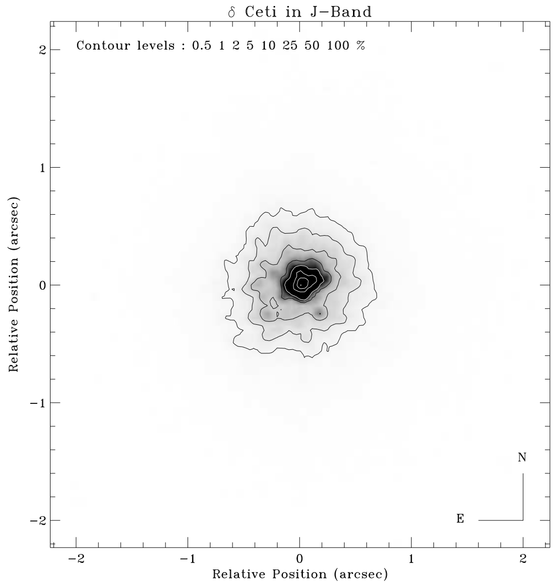

Figure 2: Shift&Add map of the point-source calibrator δ Ceti in J (total integration time of 300 s) obtained with the current adjustment of ADONIS. The lowest contour is 3 times the standard deviation of the noise.

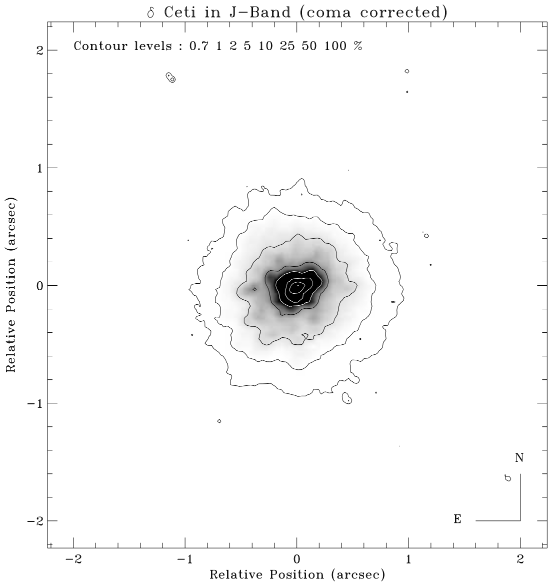

Figure 3: Shift&Add map of the point-source calibrator δ Ceti in J (total integration time of 214 s) obtained after "coma" correction. The lowest contour is 3 times the standard deviation of the noise measured at the map's corners.

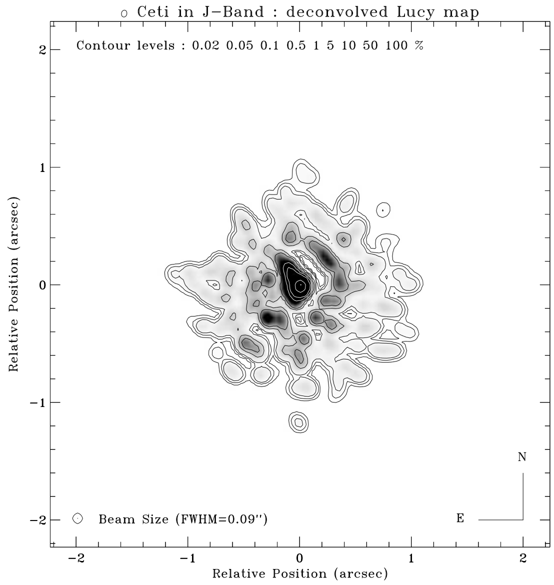

Figure 4: Deconvolved Lucy map of o Ceti in J (total integration time of 10 s) obtained with the current adjustment of ADONIS. The lowest contour is 3 times the standard deviation of the noise measured at the map's corners.

4.2 *o* Ceti

Fig.4 and Fig.5 show the deconvolved Lucy maps of o Ceti in J. Fig.4 has been obtained with the current adjustment of ADONIS. Fig.5 has been obtained after we have asked the night assistant for better correcting for residual static "coma" aberration in the IR way. Lowest contours correspond to 3 times the standard deviation of the noise measured in regions external to the envelope in the Shift&Add maps of the source. Final dynamic range is 5000:1. Angular resolution is at the diffraction limit of the 3.60-m Telescope in J. These results are discussed in more detail further in the paper.

4.3 VY CMa

Fig.6 and Fig.7 show the deconvolved Lucy maps of VY CMa respectively in J and in M. The M-map has been partially deconvolved because of the lack of flux of the point-source calibrator. Only the central part of the calibrator (including the first

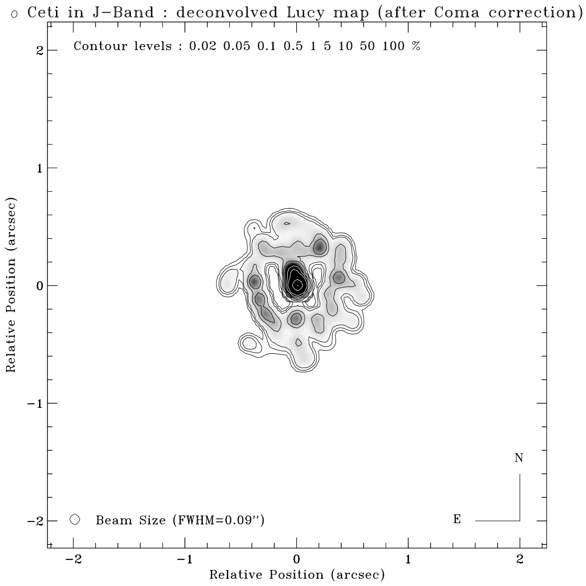

Figure 5: Deconvolved Lucy map of *o* Ceti in J (total integration time of 6 s) obtained after "coma" correction. The lowest contour is 3 times the standard deviation of the noise measured at the map's corners.

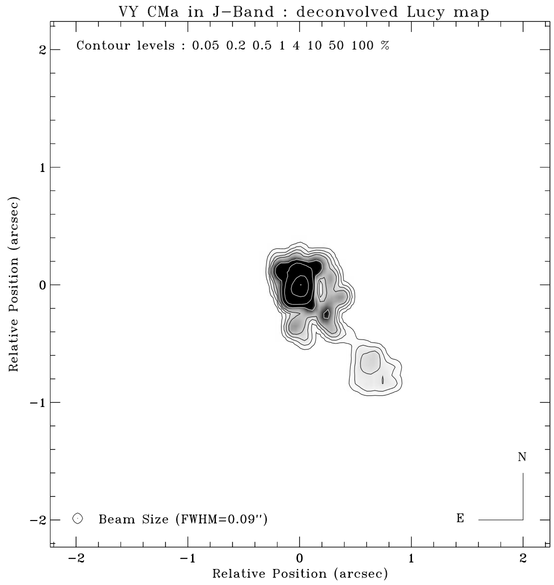

Figure 6: Deconvolved Lucy map of VY CMa in J (0.035"/pixel, total integration time of 644 s). The lowest contour is 3 times the standard deviation of the noise measured at the map's corners.

Airy ring) exceeded the background noise. Lowest contours are 3 times the standard deviation of the noise, and the dynamic range is 5000:1 in J and 2000:1 in M. Note that the scales of the maps are slightly different (0.035"/pixel in J and 0.100"/pixel in M).

4.4 V Hya and U Hya

Fig.8 and Fig.9 respectively show V Hya and U Hya in J, also deconvolved with Lucy. Again, the lowest contours are 3 times the standard deviation of the noise, but the resulting dynamic ranges of both maps are here of 10000:1.

5 Discussion

5.1 *o* Ceti

The reconstructed maps of *o* Ceti obtained with the two successive adjustments of ADONIS look quite different. The coma corrected reconstructed map appears more concentrated. However both decon-

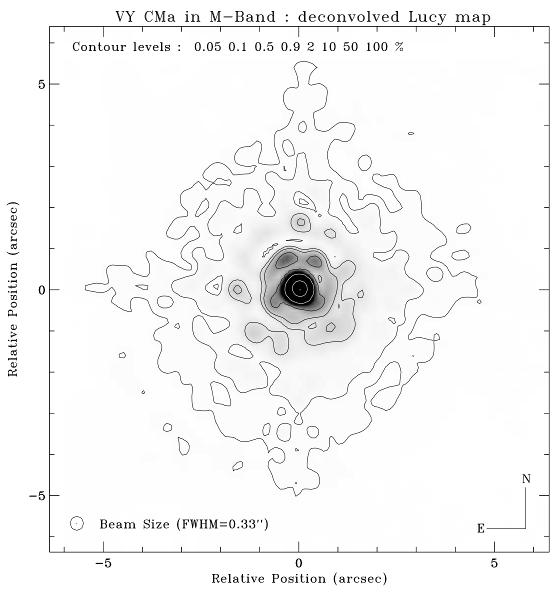

Figure 7: Partially-deconvolved Lucy map of VY CMa in M (0.1"/pixel, total integration time of 14 s). The lowest contour is 3 times the standard deviation of the noise measured at the map's corners.

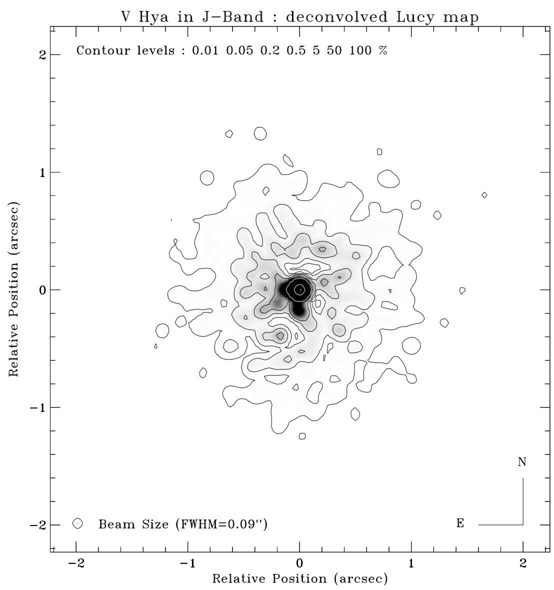

Figure 8: Deconvolved Lucy map of V Hya in J (total integration time of 67.5 s). The lowest contour is 3 times the standard deviation of the noise measured at the map's corners.

volved maps show some clumps of dust distributed on a ring centered on the star. The radius of the ring is found to be about 0.4" (i.e. about 35 R_*). The peak emission of the clumps lies between 1% and 5% of the central peak.

These reconstructed maps do not agree with our previous observations in J, H and K obtained with COME-ON+ in Sept.94 (Fig.10, Fig.11 and Fig.12). In particular, we do not confirm the suspected X-shaped structure of the shell well seen in H and K [5]. Note that the blue companion situated at $\rho = 0.61"$, $PA = 111°$ [6] is not seen in our near-infrared maps.

We could explain this misagreement by invoking at least two probable causes :

- difference of performance of COME-ON+ and ADONIS (especially in dynamic range)

- variability of the source (the phases at the two observation dates are slighly different)

On the opposite it tends to confirm the validity of the models compatible with the visibility curves at 11 μm previously obtained with ISI at Mount Wilson [7]. One of the most plausible models is based on the fact that clumps are embedded in a spherically symmetric dust shell of lower density (Fig.13 and Fig.14). We hope to confirm the ring-shaped structure of the shell with our recent HST observations completed in Aug.98.

5.2 VY CMa

Our Lucy-deconvolved J-map shows a bright knot at about 1" from the star. The peak emission of this knot lies between 0.5% and 1% of the peak flux. This feature has been previously detected in K in Sept.94 with COME-ON+ (Fig.15) [5].

The partially deconvolved M-map also shows an extension in that direction but at a peak level of 1% at a distance of 0.4" from the central core. The total integrated flux of the calibrator was not sufficient to allow high quality background substraction. Only the core (including the first Airy ring) of the calibrator could be used for deconvolution.

The direction of this extension is roughly perpendicular to the possible equatorial plane as deduced from visible observations (HST and speckle

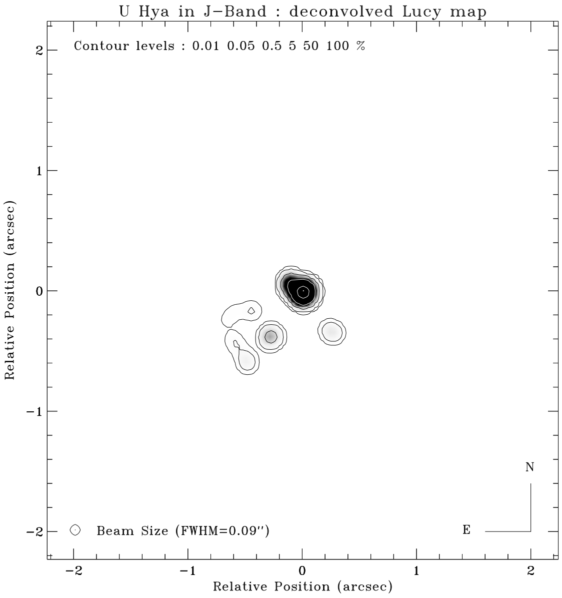

Figure 9: Deconvolved Lucy map of U Hya in J (total integration time of 67.5 s). The lowest contour is 3 times the standard deviation of the noise measured at the map's corners.

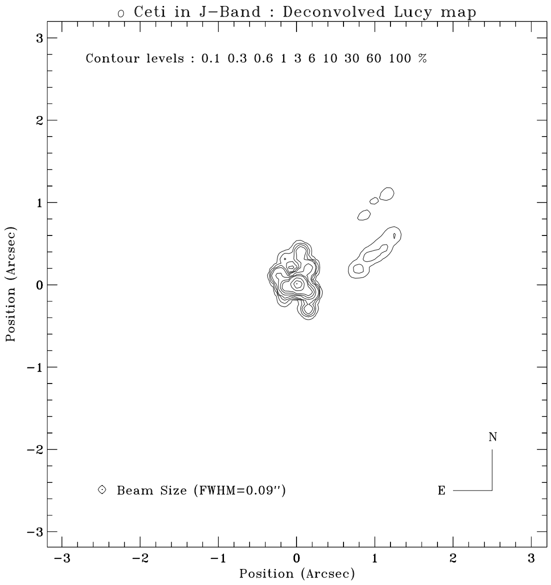

Figure 10: Deconvolved Lucy map of *o* Ceti in J obtained in Sept.94 with COME-ON+ (600 s of total integration time). Lowest contour is 0.1% of the maximum of intensity [5]

at Keck). The knot may be interpreted as light escaping from less dense polar region [8]. We can also notice that the position of the knot coincides with the predicted position of a nebulous companion, followed since 1927, compatible to a "rotating hole" hypothesis [9].

5.3 V Hya and U Hya

The Lucy-deconvolved J-map of V Hya shows a roughly spherical dust shell of 2.4" of diameter. Two clumps are detected very close to the center (at a distance inferior to 0.2") at a relative peak level of a few percents (to the East and to the South). They suggest departure from spherical geometry and could be linked to the bipolar structure proposed to explain the observations in CO lines [10].

The Lucy J-map of U Hya shows several faint well-detached knots at a peak level of 0.1% to 1% in the South-East direction, as well as a faint knot to the South-West (at a distance of 0.4"). No clear evidence for an extended dust shell has been found

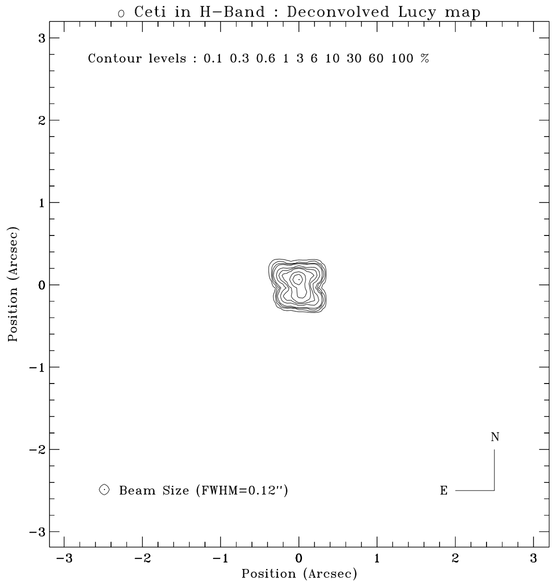

Figure 11: Deconvolved Lucy map of o Ceti in H obtained in Sept.94 with COME-ON+ (1400 s of total integration time). Lowest contour is 0.1% of the maximum of intensity [5]

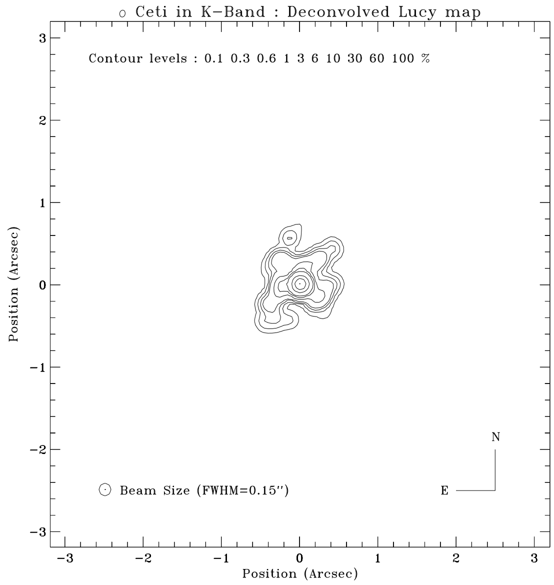

Figure 12: Deconvolved Lucy map of o Ceti in K obtained in Sept.94 with COME-ON+ (600 s of total integration time). Lowest contour is 0.1% of the maximum of intensity [5]

possibly connected to the outer ring seen at 60 μm with IRAS [11].

Acknowledgement 1 *We are grateful to the whole 3.60-m-ADONIS team that made these observations possible as well as the ESO La Silla and Garching staff for helpful assistance. We wish to specially thank Nicolas DEVILLARD from ESO-Garching for his irrepleacable help to use and maintain the ESO-ECLIPSE software. Scientific exchanges between OCA and UC Berkeley are supported by a France-Berkeley Fund grant.*

References

[1] J.-P. Lafon and N. Berruyer, "Mass loss mechanisms in evolved stars," *Astron. Astrophys. Rev.* **2**, pp. 249–289, Apr. 1991.

[2] M. Meixner, *Filling the Missing Link of Planetary Nebula Formation: A Millimeter Interferometric and Mid-IR Imaging Study of Evolved Stars.* PhD thesis, University of California at Berkeley, CA United States, 1993.

[3] M. Morris, "Mechanisms for mass loss from cool stars," *Publ. Astron. Soc. Pac.* **99**, pp. 1115–1122, Nov. 1987.

[4] I. Iben, "On the significance of mass loss from bright red giants," in *Mass Loss from Red Giants*, pp. 1–10, D. Reidel Publishing Co., (Dordrecht), June 1985.

[5] P. Cruzalèbes *et al.*, "Near-infrared adaptive optics imaging of dust shells around five late-type stars with COME-ON+," *Astron. Astrophys.* **338**, pp. 132–138, Oct. 1998.

[6] M. Karovska *et al.*, "Speckle observations of mira's companion," *Astrophys. J.* **402**, pp. 311–313, Jan. 1993.

[7] B. Lopez *et al.*, "Non-spherical structures and temporal variations in the dust shell of o ceti observed with a long baseline interferometer at 11 microns," *Astrophys. J.* **488**, p. 807, Oct. 1997.

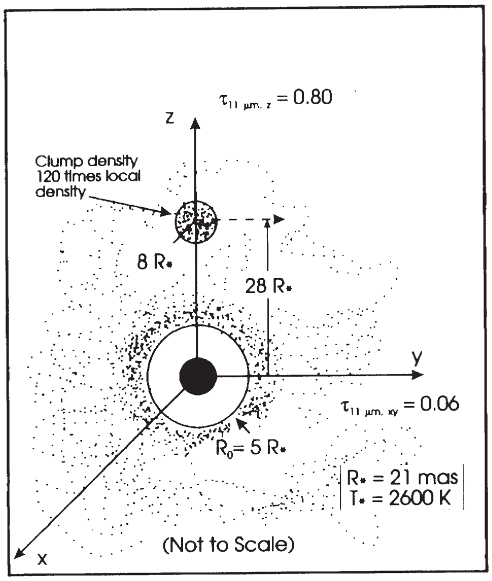

Figure 13: Schematic illustration of the model which consists of a spherical dust shell with a r^{-2} density distribution beginning at 5 R_* and an additional clump of dust 120 times as dense as the local density of dust. This clump is spherical in shape, with a radius of 8 R_*, located at a distance of 28 R_* along the z-axis from the star [7]

1989, 1993, 1994 Maxima

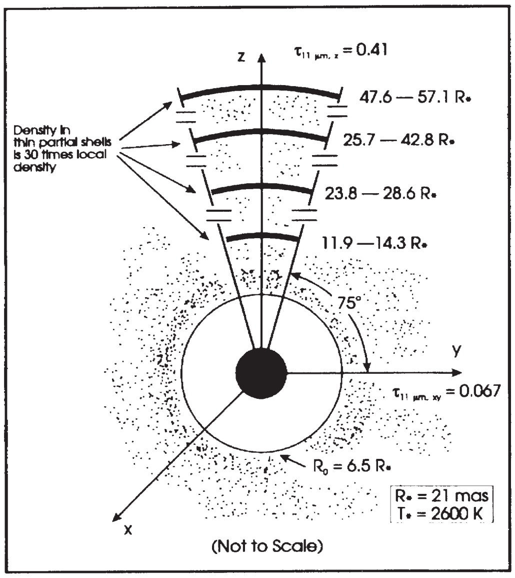

Figure 14: Schematic illustration of the model which consists of a set of spherically shaped thin dust caps, with opening half-angles of 25° as viewed from the star. The dust caps are from 11.9-14.3 R_*, 23.8-28.6 R_*, 35.7-42.8 R_*, and 47.6-57.1 R_*, respectively. The inner radius of the dust shell is at 6.5 R_*, while the optical depth along the x-y plane is 0.067 and is 0.41 along the z-axis. These clumps are embedded in a spherical dust shell and have a density 10-30 times greater than the surrounding dust [7]

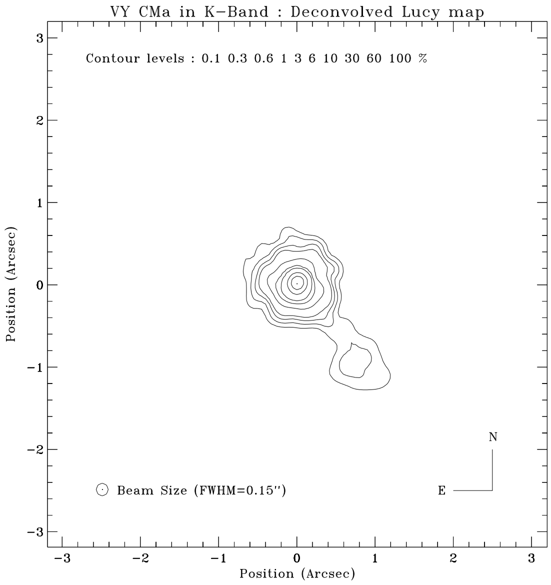

Figure 15: Deconvolved Lucy map of VY CMa in K obtained in Sept.94 with COME-ON+ (260 s of total integration time). Lowest contour is 0.1% of the maximum of intensity [5]

[8] J. Monnier *et al.*, "The last gasps of VY CMa: Aperture synthesis and adaptive optics imagery," Submitted to ApJ, July 1998.

[9] G. Wallerstein *Observatory* **98**, p. 224, 1978.

[10] C. Kahane *et al.*, "V hydrae : The missing link between spherical red giants and bipolar planetary nebulae," *Astron. Astrophys.* **314**, pp. 871–882, 1996.

[11] L. Waters *et al.*, "Resolution of a fossil dust shell around u hydrae using maximum entropy image reconstruction," *Astron. Astrophys.* **281**, pp. L1–L4, 1994.

Science Targets	**Point-source calibrators**	**Spectral type**	**IR band**	**Magnitude in IR-band**	**Exposure time**	**Number of frames**
o Ceti*		M7IIIe	J	-2.0	5 ms	2000
	δ Ceti*	B2IV	J	4.5	2 s	150
o Ceti**		M7IIIe	J	-2.0	5 ms	1200
	δ Ceti**	B2IV	J	4.5	2 s	107
VY CMa		M3/M4II	J	2.0	2 s	322
	ω CMa	B2IV-Ve	J	4.2	1 s	400
VY CMa		M3/M4II	M	-4.2	10 ms	1400
	ω CMa	B2IV-Ve	M	4.2	1 s	534
V Hya		C...	J	1.6	75 ms	900
	η Hya	B3V	J	4.7	80 ms	900
U Hya		CII...	J	1.0	75 ms	900
	η Hya	B3V	J	4.7	80 ms	900

Table 1: Journal of observations :
*Current adjustment of ADONIS
**New adjustment of ADONIS for static "coma" aberration correction